Protein engineering of a ubiquitin-variant inhibitor of APC/C identifies a cryptic K48 ubiquitin chain binding site

Edmond R. Watson[a,b], Christy R. R. Grace[a], Wei Zhang[c,d,2], Darcie J. Miller[a], Iain F. Davidson[e], J. Rajan Prabu[b], Shanshan Yu[a], Derek L. Bolhuis[f], Elizaveta T. Kulko[f], Ronnald Vollrath[b], David Haselbach[e,g], Holger Stark[g], Jan-Michael Peters[e,h], Nicholas G. Brown[a,f], Sachdev S. Sidhu[c,1], and Brenda A. Schulman[a,b,1]

[a]Department of Structural Biology, St. Jude Children's Research Hospital, Memphis, TN 38105; [b]Department of Molecular Machines and Signaling, Max Planck Institute of Biochemistry, 82152 Martinsried, Germany; [c]Donnelly Centre for Cellular and Biomolecular Research, Banting and Best Department of Medical Research, University of Toronto, Toronto, ON, Canada M5S3E1; [d]Department of Molecular Genetics, University of Toronto, Toronto, ON, Canada M5S3E1; [e]Research Institute of Molecular Pathology, Vienna BioCenter, 1030 Vienna, Austria; [f]Department of Pharmacology and Lineberger Comprehensive Cancer Center, University of North Carolina School of Medicine, Chapel Hill, NC 27599; [g]Max Planck Institute for Biophysical Chemistry, 37077 Göttingen, Germany; and [h]Medical University of Vienna, 1090 Vienna, Austria

Contributed by Brenda A. Schulman, June 24, 2019 (sent for review February 19, 2019; reviewed by Kylie Walters and Hao Wu)

Ubiquitin (Ub)-mediated proteolysis is a fundamental mechanism used by eukaryotic cells to maintain homeostasis and protein quality, and to control timing in biological processes. Two essential aspects of Ub regulation are conjugation through E1-E2-E3 enzymatic cascades and recognition by Ub-binding domains. An emerging theme in the Ub field is that these 2 properties are often amalgamated in conjugation enzymes. In addition to covalent thioester linkage to Ub's C terminus for Ub transfer reactions, conjugation enzymes often bind noncovalently and weakly to Ub at "exosites." However, identification of such sites is typically empirical and particularly challenging in large molecular machines. Here, studying the 1.2-MDa E3 ligase anaphase-promoting complex/cyclosome (APC/C), which controls cell division and many aspects of neurobiology, we discover a method for identifying unexpected Ub-binding sites. Using a panel of Ub variants (UbVs), we identify a protein-based inhibitor that blocks Ub ligation to APC/C substrates in vitro and ex vivo. Biochemistry, NMR, and cryo-electron microscopy (cryo-EM) structurally define the UbV interaction, explain its inhibitory activity through binding the surface on the APC2 subunit that recruits the E2 enzyme UBE2C, and ultimately reveal that this APC2 surface is also a Ub-binding exosite with preference for K48-linked chains. The results provide a tool for probing APC/C activity, have implications for the coordination of K48-linked Ub chain binding by APC/C with the multistep process of substrate polyubiquitylation, and demonstrate the power of UbV technology for identifying cryptic Ub-binding sites within large multiprotein complexes.

anaphase-promoting complex | APC/C | ubiquitin | E3 ligase | inhibitor

Posttranslational modification by ubiquitin (Ub) regulates numerous eukaryotic cellular processes, including cell division, signal transduction, transcription, translation, protein trafficking, and more. The exceptional regulatory potential of the Ub system stems from both a vast enzymatic system that links Ub to specific protein targets and enormous diversity in forms of ubiquitylation. Ub is not a singular modification, but is often itself modified by additional Ubs in the form of "chains," where Ubs are linked via one of 8 different primary amino groups (lysine side chains or the N terminus) on another Ub. Precise ubiquitylation is catalyzed by specific combinations of E3 Ub ligases and E2 Ub-conjugating enzymes, and the resultant Ub marks are recognized by Ub-binding domains that impart distinct fates to modified proteins (1–8). As examples, K11- and K48-linked Ub chains, particularly in combination with each other, elicit proteasomal degradation, whereas K63-linked chains often modulate subcellular location or assembly and disassembly of macromolecular complexes.

E3 enzymes achieve ubiquitylation by recruiting single or more sequence motifs, termed "degrons," in a substrate and promoting Ub transfer through one of various mechanisms determined by the type of catalytic domain. E3s harboring "HECT" and "RBR" catalytic domains promote ubiquitylation through 2-step reactions involving formation of a thioester-linked intermediate between the E3 and Ub's C terminus: First, Ub is transferred from an E2~Ub intermediate ("~" refers to thioester bond) to the E3 catalytic Cys; Ub is subsequently transferred from the E3's Cys to the substrate (9–13). Alternatively, the majority of E3s, including an estimated ~500 RING E3s in humans, do not directly relay Ub themselves but, instead, activate Ub transfer from the catalytic Cys of a Ub-carrying enzyme, which is typically an E2 but can also

Significance

Ubiquitin (Ub)-mediated interactions influence numerous biological processes. These are often transient or a part of multivalent interactions. Therefore, unmasking these interactions remains a significant challenge for large, complicated enzymes such as the anaphase-promoting complex/cyclosome (APC/C), a multisubunit RING E3 Ub ligase. APC/C activity regulates numerous facets of biology by targeting key regulatory proteins for Ub-mediated degradation. Using a series of Ub variants, we identified a new Ub-binding site on the APC/C that preferentially binds to K48-linked Ub chains. More broadly, we demonstrate a workflow that can be exploited to uncover Ub-binding sites within ubiquitylation machinery and other associated regulatory proteins to interrogate the complexity of the Ub code in biology.

Author contributions: E.R.W., C.R.R.G., D.J.M., H.S., J.-M.P., N.G.B., S.S.S., and B.A.S. designed research; E.R.W., C.R.R.G., W.Z., D.J.M., I.F.D., J.R.P., S.Y., D.L.B., E.T.K., R.V., D.H., and N.G.B. performed research; E.R.W., C.R.R.G., W.Z., D.J.M., I.F.D., J.R.P., H.S., J.-M.P., N.G.B., S.S.S., and B.A.S. contributed new reagents/analytic tools; E.R.W., C.R.R.G., D.J.M., J.R.P., J.-M.P., N.G.B., S.S.S., and B.A.S. analyzed data; and E.R.W., C.R.R.G., D.J.M., N.G.B., and B.A.S. wrote the paper.

Reviewers: K.W., National Cancer Institute; and H.W., Harvard Medical School.

The authors declare no conflict of interest.

Data deposition: Coordinates and structure factors for UbVW (PDB ID code 6NXL), ubiquitin bound to APC2 WHB (PDB ID code 6NXK), and coordinates, structure factors, and NMR chemical shifts for UbVW_dim bound to APC2 WHB (PDB ID code 6OB1) can be accessed from the Protein Data Bank, www.wwpdb.org. The cryo-electron microscopy map reported in this paper has been deposited in the Electron Microscopy Data Bank (accession code EMD-10072).

See Commentary on page 17142.

[1]To whom correspondence may be addressed. Email: sachdev.sidhu@utoronto.ca or schulman@biochem.mpg.de.

[2]Present address: Department of Molecular and Cellular Biology, College of Biological Science, University of Guelph, Guelph, ON, Canada N1G2W1.

This article contains supporting information online at www.pnas.org/lookup/suppl/doi:10.1073/pnas.1902889116/-/DCSupplemental.

Published online July 26, 2019.

be a thioester-forming E3 (14, 15). Notably, many RING E3s are multifunctional, interacting with several distinct Ub-carrying enzymes to link various forms of Ub to myriad substrates. In many cases, a substrate undergoes polyubiquitylation by different combinations of enzymes acting in series. For example, some RING E3s employ different E2s, with one first priming a substrate directly with Ub and then the other extending Ub chains from substrate-linked Ubs (16, 17).

Recent studies have shown that the catalytic domains of several E3 and E2 enzymes not only carry Ub covalently at their active sites to mediate ubiquitylation but also bind Ub noncovalently at "exosites" remote from their hallmark catalytic surfaces (18). Noncovalent Ub binding can influence targeting, processivity, and rates of ubiquitylation reactions. As examples, noncovalent Ub binding to the E2 UBE2D2 allosterically modulates binding to partner RING domain E3s (19, 20), while noncovalent binding to HECT E3s in the NEDD4 family can modulate catalytic activity and/or processivity of substrate ubiquitylation (21). The first RING domain discovered to possess a Ub-binding exosite was APC11, a subunit of one of the most complicated and unusual E3 ligases, the anaphase-promoting complex/cyclosome (APC/C) (22). APC/C, a 1.2-MDa complex composed of 19 core polypeptides, including APC11 and the cullin-like APC2, controls cell division by promoting Ub-dependent turnover of cyclins and other key cell cycle regulators (reviewed in refs. 23, 24). Recent structural studies have revealed how APC/C is activated through binding to a coactivator (either CDC20 or CDH1), which recruits substrate degrons and conformationally activates the APC2-APC11 cullin-RING catalytic core (25), and how the APC2-APC11 catalytic core, in turn, differentially recruits and activates distinctive E2∼Ub intermediates to generate various ubiquitylated products (26–28). Human APC/C employs the E2 UBE2C to prime substrates with 1 or multiple individual Ubs or short poly-Ub chains, as well as the E2 UBE2S to extend chains with K11 linkages (29–32). When UBE2S encounters substrates modified with K48-linked Ub chains generated by UBE2C, "branched" chains containing K48 and K11 linkages are produced, which are particularly potent at directing proteasomal degradation (33).

APC11's Ub-binding exosite makes distinct contributions to the reactions with the different E2s (Fig. 1*A*). With UBE2C, in a process called "processive affinity amplification," this exosite provides additional affinity for Ub-linked substrates, which increases the propensity for further modification (28, 34). In a different, crucial role in APC/C-dependent polyubiquitylation with UBE2S, APC11's Ub-binding exosite recruits substrate-linked Ubs for K11-linked Ub chain elongation (22, 35). In addition to the key roles played by Ub binding to APC11, single-molecule studies indicated the presence of other, unidentified, Ub-binding sites on APC/C (28).

Although it is of great interest to identify Ub-binding domains, it can be challenging to find these interactions de novo. One obstacle is that the affinities of interactions between Ub and binding domains are typically extremely low, with dissociation constants (K_ds) often in the millimolar range (36). Such low affinities generally reflect a single Ub being only one of many elements contributing to avid, multisite interactions (37). As a consequence, many Ub-binding sites have been identified by yeast 2-hybrid pulldowns or NMR experiments with high concentrations of interacting domains. However, in the absence of sequence motifs indicating the presence of a Ub-binding domain, it is an arduous task to find such interactions within massive assemblies that cannot be produced in large quantities at high concentrations for techniques such as NMR. Indeed, we previously discovered the Ub-binding exosite fortuitously, through alanine-scanning mutagenesis of APC11's RING domain and assaying enzymatic activity with UBE2S in the context of the fully assembled, recombinant >1.2-MDa APC/C^{CDH1} complex (22).

We considered that it might be possible to use "Ub variant" (UbV) technology to identify a new Ub-binding site within APC/C. Unlike Ub, which is constrained in sequence and structure by the requirement to bind a massive number of partner proteins, sequence variants have the potential to make distinctive contacts that increase affinity for particular partners. We and others previously performed phage display to select variants binding to a variety of E3 ligases and deubiquitylating enzymes (DUBs), as well as previously identified Ub-binding domains, to test effects of perturbing Ub interactions with known interaction sites (21, 28, 38–44). Indeed, our UbV^{R}, selected from among 10^{10} UbVs displayed on phage as binding APC11's RING domain, proved useful for uncovering the contribution of APC11's Ub-binding exosite to processive affinity amplification of activity with UBE2C, and enabled obtaining cryo-electron microscopy (cryo-EM) data visualizing UBE2S bound to the APC2-APC11 catalytic core of APC/C (28).

Here, we utilize UbV technology with a different goal: We tested for perturbation of E3 activity without prior knowledge of a specific Ub-binding site. In so doing, we generated an inhibitor of substrate priming by UBE2C that stabilizes APC/C targets in mitotic extracts. Remarkably, this strategy also identified the UBE2C-binding site on the APC2 cullin domain as a previously unknown Ub-binding exosite with preference for K48-linked chains. The results have implications for the interplay between polyubiquitylated substrates, E2s, and other factors regulating APC/C activity through interactions with the cullin subunit. Furthermore, we provide a route for identifying novel Ub-binding sites within massive multiprotein assemblies.

Results

Identification of a UbV Inhibiting Ub-Mediated Proteolysis of APC/C-UBE2C Substrates. During the course of characterizing effects of UbV^{R}, which binds APC11's RING domain with ≈1 μM affinity, we monitored APC/C^{CDH1}-catalyzed ubiquitylation in the presence of excess individual UbVs from a panel of purified proteins available in the laboratory. UBE2C-dependent substrate priming and UBE2S-dependent Ub chain-extending activities (Fig. 1*A*) were assayed in parallel using the model substrate "UbCycBNT*," consisting of Ub fused upstream of the N-terminal domain of cyclin B, which contains a D-box "degron," and a C-terminal fluorophore. In the control reactions recapitulating our prior results (28), UbV^{R} decreased processivity with UBE2C, as shown by conversion of substantial substrate to products with fewer Ubs (Fig. 1*B*). In addition, all activity with UBE2S is impaired by UbV^{R} competing with the acceptor Ub for binding to the APC11 RING domain. Most UbVs had little effect on either reaction, which was not surprising, given that none of them were selected specifically for binding to domains from APC/C^{CDH1}. Serendipitously, however, a single UbV (termed UbV^{W}, for reasons described below) displayed a distinctive profile: selective inhibition of reactions with UBE2C with no obvious effect on polyubiquitylation with UBE2S (Fig. 1*B*). Relative to wild-type Ub (45), UbV^{W} displays mutations primarily in the "Leu8 loop" between the 2 N-terminal β-strands and in the C-terminal tail, and retains the I44 hydrophobic patch known to mediate most interactions, albeit with L8V, H68I, and V70L substitutions (Fig. 1 *C* and *D*).

Consistent with the notion that UbV^{W} specifically antagonizes APC/C with UBE2C, reactions with relatively higher concentrations of UBE2C showed increased ubiquitylation, which were attenuated by the presence of UbV^{W} (Fig. 1*E*). An additional UbV selected as a negative control (UbV^{Neg}) showed no effect on these reactions, and excess UBE2C alone does not catalyze ubiquitylation in the absence of APC/C.

To evaluate APC/C and UBE2C activity in a more physiological setting, we examined effects of UbV^{W} on degradation of well-characterized substrates, cyclin B1 and Securin, in mitotic *Xenopus* egg extracts. These extracts were previously shown to

retain key cellular requirements for APC/C-dependent degradation during the cell cycle, including substrate priming activity from collaboration with endogenous UBE2C present in the extracts (29, 46, 47). Importantly, addition of UbV^{W}, but not UbV^{Neg}, stabilized the cell cycle proteins from APC/C-UBE2C–dependent degradation (Fig. 1*F*).

UbV^{W} Hijacks APC2's WHB Domain to Compete with Binding to UBE2C. To gain mechanistic insights into how UbV^{W} could selectively inhibit APC/C activity with UBE2C, we performed kinetic analyses. Adding saturating concentrations of UbV^{W} while titrating UBE2C caused a 5-fold increase in the Michaelis constant (K_m), with only a minor effect on the maximum velocity (Fig. 2*A*), implying that UbV^{W} antagonizes UBE2C binding to APC/C.

Three potential explanations for this result are suggested from prior structures of UBE2C bound to APC/C (26, 27) (Fig. 2*B*). First, UbV^{W} could bind directly to UBE2C to compete with APC/C binding. Second, UbV^{W} could block the canonical E2-binding site on the APC11 RING domain. Third, UbV^{W} could prevent the distinctive recruitment of UBE2C that is mediated by the so-called "WHB domain" from APC2. To distinguish between these possibilities, we performed NMR experiments examining the effects on [^{15}N-^{1}H] transverse relaxation-optimized spectroscopy (TROSY) or heteronuclear single quantum coherence spectroscopy (HSQC) spectra when UbV^{W} was added to [^{15}N]-labeled versions of UBE2C, APC11 RING domain, or APC2 WHB domain. Only the latter spectrum showed substantial chemical shift perturbations, indicating that UbV^{W} binds directly to the WHB domain from APC2 (Fig. 2*C*). Indeed, a K_d of ~1.7 μM was measured by biolayer interferometry upon titrating UbV^{W} with immobilized glutathione *S*-transferase (GST)-APC2 WHB (Fig. 2*D*). Hence, the name UbV^{W} reflects binding to APC2's WHB domain. Interestingly, the APC2 WHB was already known to be a multifunctional protein interaction domain. In addition to its role in recruiting UBE2C to catalyze substrate ubiquitylation, this domain binds the BUBR1 subunit of the mitotic checkpoint complex (MCC) during APC/C inhibition from the spindle assembly checkpoint (48, 49).

An in vitro ubiquitylation assay with opposing inhibitors was used to further test if UbV^{W} competing with UBE2C for APC2's WHB domain is responsible for the inhibition of APC/C activity. UBE2C-dependent ubiquitylation of a substrate (fluorescent cyclin B N-terminal domain [CycBNT*]) is inhibited both by UbV^{W}, which presumably binds the APC2 WHB domain in context of the APC/C^{CDH1} complex, and by the isolated APC2 WHB domain, which binds UBE2C and prevents its binding to APC/C (27). However, adding UbV^{W} partially ameliorated the inhibition exerted by the isolated APC2 WHB domain, consistent with UbV^{W} binding, in effect, liberating UBE2C to perform ubiquitylation (Fig. 2*E*). Taken together, the results indicate that UbV^{W} binds APC2's WHB domain within the APC/C^{CDH1} complex in a manner that competes with the binding of UBE2C.

A Domain-Swapped Dimer Structure Enables UbV^{W} to Bind the APC/C with High Affinity. As a first step toward understanding the structural basis for its effects, we determined a crystal structure of UbV^{W} at a resolution of 2.8 Å (*SI Appendix*, Table S1). The structure revealed 2 striking features. First, the crystal contains an oligomeric crystal packing assembly with 8 copies in the asymmetric unit (Fig. 3*A*). Analytical ultracentrifugation and size exclusion chromatography-multiangle light scattering (SEC-MALS) confirmed a higher order oligomer (tetramer) in solution (Fig. 3*B* and *SI Appendix*, Fig. S1*A*). Second, the model revealed that the UbV forms a symmetric domain-swapped dimer where the normal Ub β1-β2 loop composed of residues 6 to 9 is extended such that the β1 strand from one subunit forms an

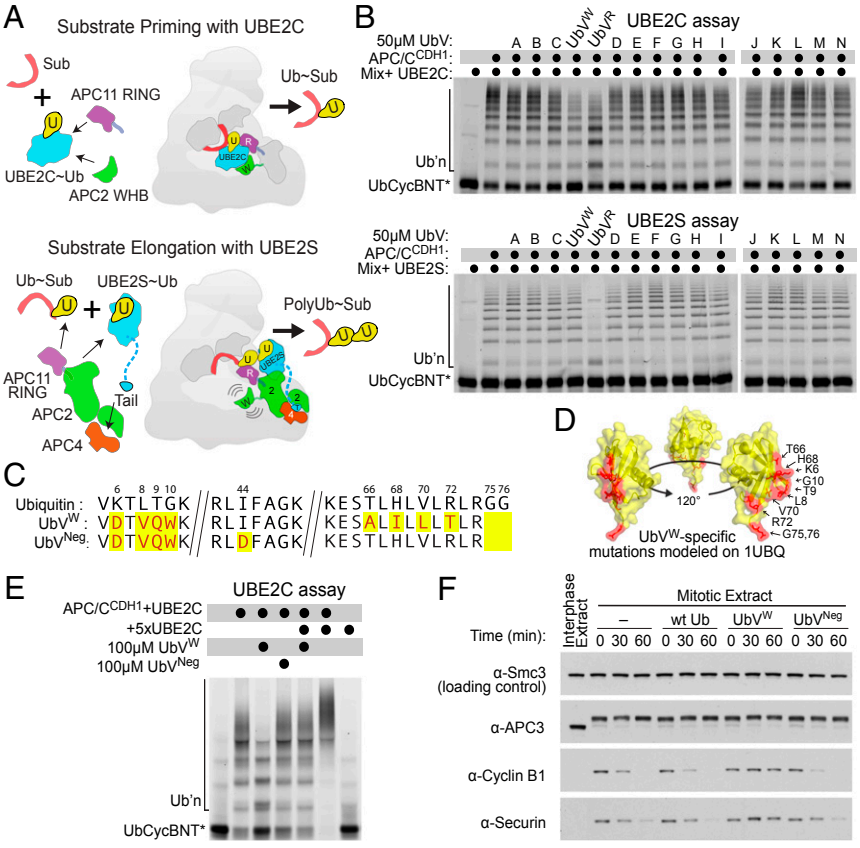

Fig. 1. Discovery of a UbV inhibitor (UbV^{W}) of APC/C activity with UBE2C. (*A*) Cartoons illustrating the distinct APC/C ubiquitylation mechanisms. (*Top*) In a substrate priming reaction, UBE2C (cyan) is harnessed by APC2 WHB (green) and the canonical APC11 RING residues (purple) to catalyze transfer of Ub (yellow) to substrate (red). (*Bottom*) In a Ub chain elongation reaction, UBE2S is harnessed at a distal site and utilizes distinct surfaces of APC2 (green), APC4 (orange), and APC11 (purple) to generate poly-Ub chains on existing Ub conjugates (yellow). (*B*) Panel of UbV proteins was assayed for effects on ubiquitylation using Ub-fusion to the fluorescent cyclin B N-terminal domain (UbCycBNT*), an APC/C^{CDH1} substrate suitable for modification by both the substrate-priming E2 UBE2C (*Top*) and the Ub chain-elongating E2 UBE2S (*Bottom*). Ubiquitylated products are separated via 15% sodium dodecyl sulfate polyacrylamide gel electrophoresis and visualized in a Typhoon biomolecular fluorescence imager. Ub'n, ubiquitin conjugated to UbCycBNT*. (*C*) Sequence alignment of Ub, UbV^{W}, and control mutant UbV^{Neg}, with divergent residues highlighted in yellow. (*D*) Sequence divergence in UbV^{W} is shown in red, mapped on the structure of Ub (Protein Data Bank ID code 1UBQ). (*E*) Ubiquitylation of UbCycBNT* is monitored in the presence of excess UBE2C, UbV^{W}, or control mutant UbV^{Neg}. UbV^{W} inhibits in the presence of excess UBE2C, suggesting indirect inhibition. (*F*) Effects of UbV^{W}, wild-type (wt) Ub, or UbV^{Neg}, on degradation of exogenous APC/C substrates cyclin B1 and Securin in extracts from mitotic *Xenopus* eggs, monitored by Western blot. Antibody specificities are denoted to the left, with SMC3 as a loading control and the slower migrating phosphorylated APC3 indicating active APC/C in the extracts.

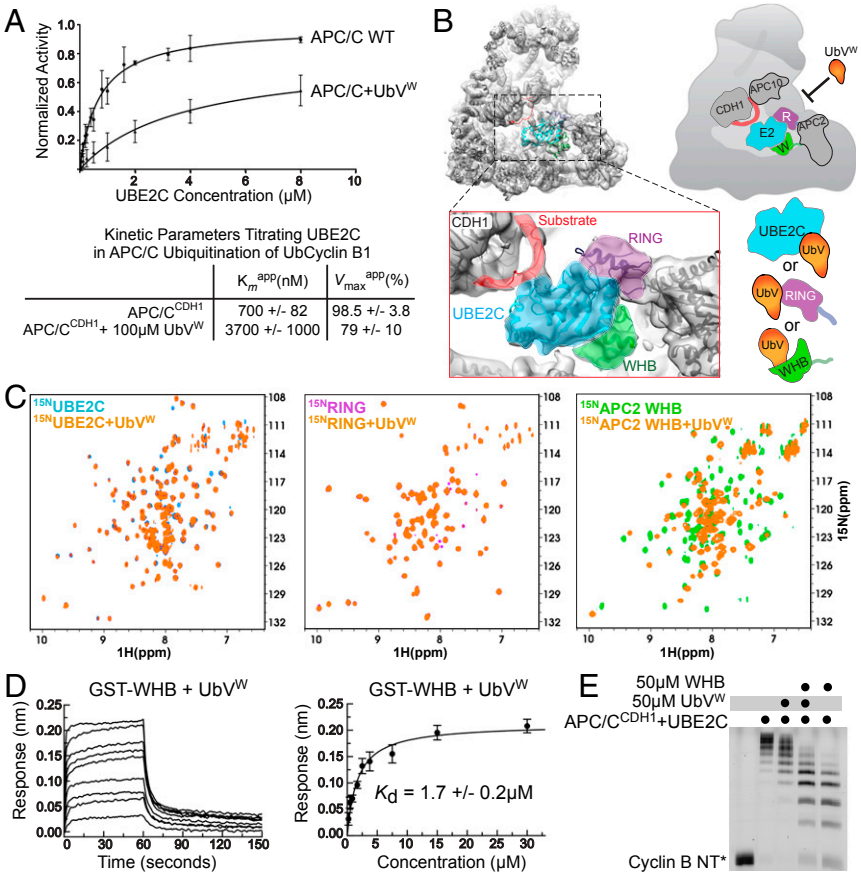

Fig. 2. UbV^{W} directly interacts with APC/C to antagonize UBE2C activity. (*A*) Curve fits (*Top*) and kinetic parameters (*Bottom*) testing effects of saturating UbV^{W} on titrations of UBE2C in APC/C^{CDH1}-mediated ubiquitylation of Ub fusion to fluorescent cyclin B N-terminal domain (UbCycBNT*). SEM ($n \geq 3$). WT, wild type. (*B*, *Left*) Potential mechanisms of UbV^{W} inhibition of APC/C activity with UBE2C, based on a prior EM map (Electron Microscopy Data Bank accession code 3432 [28]) of UBE2C bound to APC/C^{CDH1} substrate, with a close-up view of substrate (red), UBE2C (cyan), APC11 RING (purple), and APC2 WHB domain (green). (*B*, *Right*) Cartoons illustrating 3 possible mechanisms for UbV inhibition of UBE2C recruitment by associating with UBE2C directly, with APC11 RING domain, or with APC2 WHB domain. (*C*, *Left*) Overlaid [^{15}N-^{1}H] TROSY spectra of [^{15}N]-labeled UBE2C alone (100 μM, cyan) or with UbV^{W} (1:2, orange). (*C*, *Middle*) Overlaid [^{15}N-^{1}H] TROSY spectra of [^{15}N]-labeled APC11 RING alone (100 μM, purple) or with UbV^{W} (1:2, orange). (*C*, *Right*) Overlaid [^{15}N-^{1}H] HSQC spectra of [^{15}N]-labeled APC2 WHB alone (100 μM, green) or with UbV^{W} (1:2, orange). ppm, parts per million. (*D*) Representative sensorgram and curve fit for binding measured by bio-layer interferometry with UbV^{W} titrated in solution versus immobilized GST-APC2 WHB domain. SEM ($n \geq 2$). (*E*) Ubiquitylation of fluorescent cyclin B N-terminal domain (CycBNT*) by APC/C and UBE2C is monitored in the presence of UbV^{W}, excess isolated WHB domain, or a combination of both inhibitors. Alleviation of inhibition when UbV^{W} and isolated WHB are used in combination suggests direct binding.

antiparallel β-sheet with the opposite subunit (Fig. 3*C*). In this arrangement, we refer to a "monomer" as the portion of the dimer corresponding to the Ub-like fold and the residues involved in the domain swap. This comprises residues 1 to 10 of one protomer (A) and residues 8 to 74 of the opposite protomer (B) in the domain-swapped dimer, where Val8 of protomer A indirectly stabilizes the fold and Val8-Trp10 of both protomers form the β-sheet extension mediating the domain swap. The globular portion (residues 1 to 70) of the "monomer" superimposes on the corresponding portion of Ub (residues 1 to 70) with 1.2-Å backbone root-mean-square deviation.

Interestingly, the domain-swapping of UbV^{W} is reminiscent of that recently reported for other UbVs, one that binds the dimeric RING-RING assembly from the E3 XIAP (UbV.XR) and another that binds the DUSP domain of the DUB USP15 (UbV.15.D) (42, 50). Conformational differences between 2 independent crystal structures of UbV.XR suggested flexibility in the β-sheet formed by the domain swap, with different relative orientations varying by 30° for the 2 halves of the dimer. Superimposition of a monomer of UbV^{W} reveals yet a different arrangement, raising the possibility that domain-swapped UbVs will generally display flexibility across the dimer interface (Fig. 3*D*).

The NMR spectrum of UbV^{W} was examined for potential dynamic behavior. Indeed, extreme line broadening and multiple peaks indicative of slow exchange between multiple interconverting conformations precluded resonance assignment for UbV^{W} alone. Nonetheless, assignments of [^{13}C-^{15}N] UbV^{W} in the presence of the APC2 WHB domain, and vice-versa, enabled identifying intermolecular nuclear Overhauser effect (NOE) data, which suggested that the interaction centers around UbV^{W} residues corresponding to Ub's canonical hydrophobic patch and the UBE2C-binding site on the APC2 WHB. However, residual conformational dynamics precluded structure calculation for the UbV^{W}/APC2 WHB complex.

To determine whether features of the domain swap were essential for the interaction, we examined sequences of the known UbVs displaying domain swaps. Notably, UbV^{W}, UbV.XR, and UbV.15.D harbor replacements for Ub's residue Gly10, raising the possibility that Gly10 is important for maintaining a monomeric Ub fold structure. Reverting Trp10 to Gly indeed yielded a monomer in solution as determined by analytical ultracentrifugation and SEC-MALS (Fig. 3*B* and *SI Appendix*, Fig. S1 *A* and *B*), but also eliminated the interaction with APC2's WHB domain (Fig. 3*E*). Although more conservative replacements for

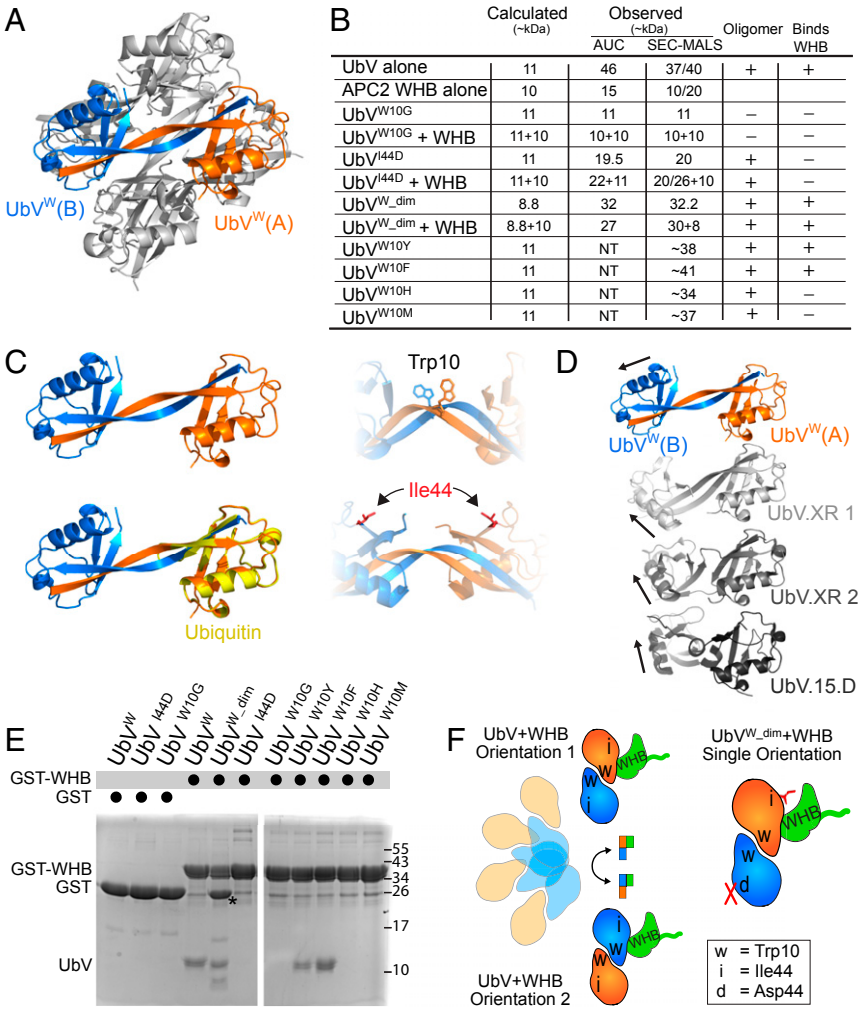

	Calculated (~kDa)	Observed (~kDa) AUC	Observed (~kDa) SEC-MALS	Oligomer	Binds WHB
UbV alone	11	46	37/40	+	+
APC2 WHB alone	10	15	10/20		
UbV^{W10G}	11	11	11	–	–
UbV^{W10G} + WHB	11+10	10+10	10+10	–	–
UbV^{I44D}	11	19.5	20	+	–
UbV^{I44D} + WHB	11+10	22+11	20/26+10	+	–
UbV^{W_dim}	8.8	32	32.2	+	+
UbV^{W_dim} + WHB	8.8+10	27	30+8	+	+
UbV^{W10Y}	11	NT	~38	+	+
UbV^{W10F}	11	NT	~41	+	+
UbV^{W10H}	11	NT	~34	+	–
UbV^{W10M}	11	NT	~37	+	–

Fig. 3. Structure of UbV^{W} reveals a dynamic association with APC/C and necessitates UbV^{W_dim} to stabilize a single conformation upon binding. (*A*) Crystal structure of UbV^{W}, determined to a resolution of 2.8 Å, reveals an oligomeric assembly. Two copies of UbV represent the biological unit, colored in orange (UbV^{W} protomer A) and blue (UbV^{W} protomer B). (*B*) Summary of the results of biophysical analyses of purified UbV mutants and APC2 WHB domain. Wild-type and mutant versions of UbV^{W} were analyzed by sedimentation velocity analytical ultracentrifugation (AUC) and SEC-MALS, either as purified apo proteins or in combination with APC2 WHB domain. (*C*, *Top Left*) Isolated homodimer of UbV^{W} from the oligomeric assembly showing protomer A (orange) and protomer B (blue) interacting as a β-strand–swapped dimer, representing the biological unit. (*C*, *Bottom Left*) Composite "monomer" of the UbV^{W} structure superimposes well with Ub. (*C*, *Right*) Notably, the dimer contains 2 copies of residues shown to be involved in the interaction with APC/C, including Trp10 and Ile44. (*D*) Comparison of UbV^{W} with previously reported domain-swapped dimeric UbVs (UbV.XR and UbV.15.D) reveals a structural relationship; each harbors mutations to amino acid 10, which enables strand-swapping and conformational flexibility between the protomers. (*Top*) UbV from this study with protomer A in orange and protomer B in blue. (*Middle*) Published UbV.XR shown in light (Protein Data Bank [PDB] ID code 5O6S [42]) or medium (PDB ID code 5O6T [42]) gray when aligned over protomer A. (*Bottom*) Published UbV.15.D (PDB ID code 6DJ9 [50]) shown in dark gray when aligned over protomer B. Arrows trace the path of the α-helix within protomer B. (*E*) Selected mutants of UbV^{W} are assessed for association with an immobilized GST-APC2 WHB, with purified GST alone serving as a negative control. An asterisk denotes degradation product from residual tobacco etch virus protease in the UbV^{W_dim} preparation. (*F*) Model demonstrating dynamic association between 2 copies of UbV^{W} per APC/C (*Left*) or stable association of UbV^{W_dim} harboring a single Ile44 mutation per dimer, rendering 1 copy inefficient at binding APC/C (*Right*).

Trp10 to Phe, Tyr, His, or Met failed to prevent oligomerization, His and Met substitutions did block assembly with APC2 (Fig. 3*B* and *SI Appendix*, Fig. S1*C*). Thus, Trp10 is not only essential for the domain swap but apparently plays a role in mediating UbV^{W} binding to APC2.

To facilitate structure determination, we sought to generate a more uniform domain-swapped UbV that retains Trp10, adopts a dimer without higher order self-association, and forms a singular assembly with the APC2 WHB domain. An I44D mutant UbV satisfied the criterion of forming a dimer, presumably maintaining the strand swap and ablating further self-association, but did not bind APC2 (Fig. 3 *B* and *E*). However, following coexpression of a His-tagged UbV^{W} with a GST-tagged I44D mutant, tandem affinity chromatography yielded a heterodimeric domain-swapped dimer that binds APC2 with improved properties (Fig. 3 *B*, *E*, and *F*). We term this engineered dimer $UbV^{W\text{-}dim}$, with protomer "A" retaining Ile44 and protomer "B" harboring the I44D mutation.

Structural Mechanism of UbV Inhibition of APC/C Substrate Ubiquitylation by UBE2C. $UbV^{W\text{-}dim}$ retains the original interaction with the APC2 WHB domain, as indicated by nearly identical chemical shift perturbations when UbV^{W} and $UbV^{W\text{-}dim}$ are added to [^{15}N]-labeled APC2 WHB domain (Fig. 4*A* and *SI Appendix*, Fig. S2*A*) and its ability to inhibit UBE2C-mediated ubiquitylation and bind APC2 WHB directly, albeit with reduced affinity attributable, in part, to the now defunct protomer B (*SI Appendix*, Fig. S2 *B* and

C). Furthermore, the improved NMR spectral properties enabled structure determination for the UbV^{W_dim} complex with APC2 WHB (Fig. 4*B* and *SI Appendix*, Fig. S2 *E* and *F* and Table S2). Representative structures converge to show the same interactions between 1 Ub-like fold, or "monomer", of UbV^{W_dim} and the APC2 WHB domain, with variable placement of the second Ub-like fold in the domain-swapped dimer (Fig. 4*C*). Flexibility is apparently imparted by the residues surrounding and including Val8′ to Ile13′ ("′" refers to side chains from protomer B), as this region displayed particularly broad spectra and the Cα plot for this region differs from that of Ub (*SI Appendix*, Fig. S2*G*). With the exception of the side chains of Val-8 and Trp-10 located in the strand-swap, this latter Ub-like fold of the dimer does not participate in the interaction and is not discussed further. Rather, we focus on the convergent interactions between a single Ub-like fold domain from UbV^{W_dim} and APC2, which bury ~700 Å^2 of total surface area.

As with many complexes with Ub, the interaction is largely hydrophobic, with intermolecular NOEs centering around the UbV^{W} residues corresponding to Ub's canonical hydrophobic patch (here, Val8, Ile44, Ile68, and Leu70) and the first and second helices and intervening loop of APC2's WHB domain

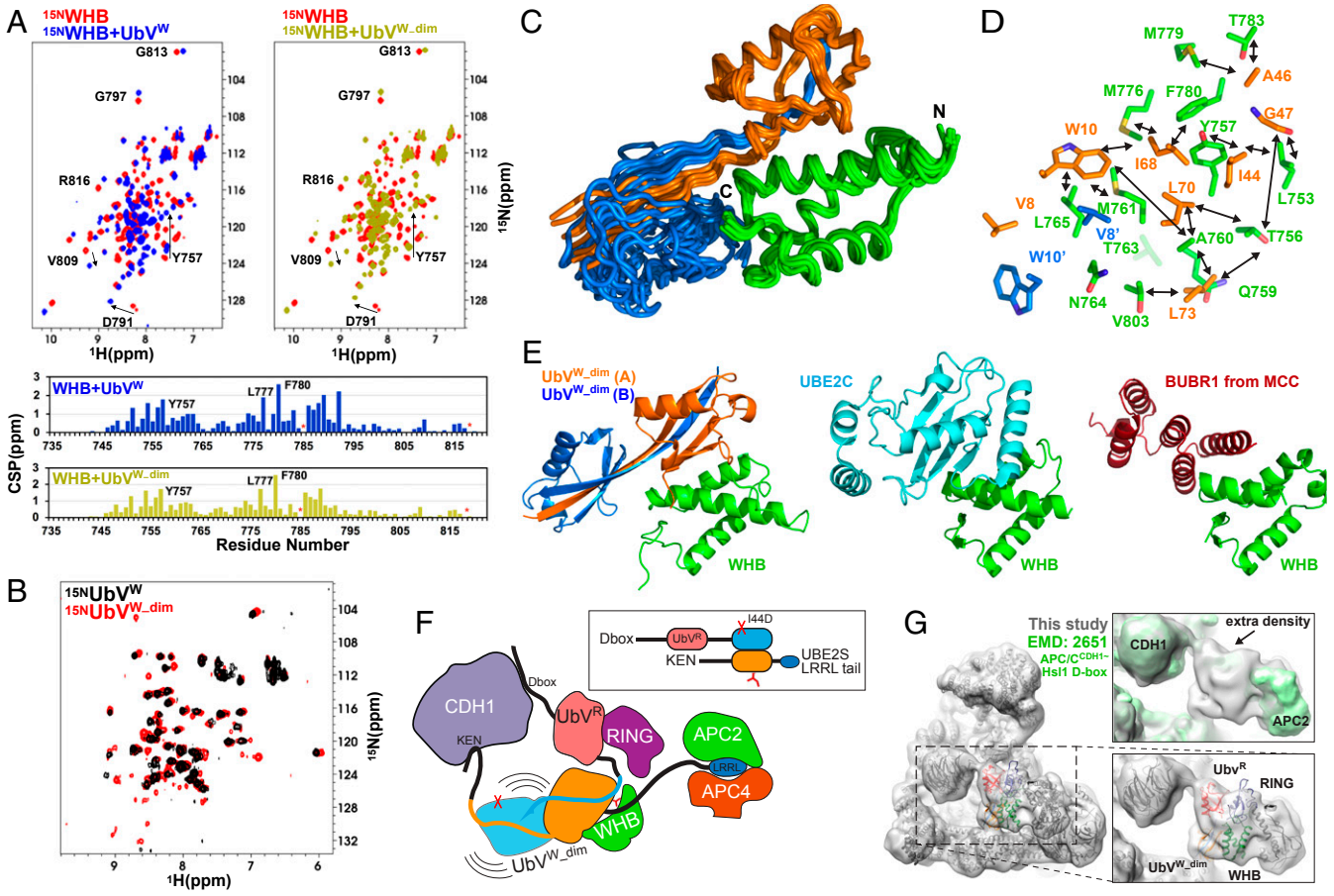

Fig. 4. Structure of UbV^{W_dim} bound to APC2 WHB domain reveals the molecular basis for blocking UBE2C. (*A*, *Left Top*) Overlaid [^{15}N-^{1}H] HSQC spectra of [^{15}N]-labeled APC2 WHB alone (100 μM, red) or with UbV^{W} (1:2, blue) with corresponding Chemical Shift Perturbation (CSP) analysis shown below (blue). (*A*, *Right Top*) Overlaid [^{15}N-^{1}H] HSQC spectra of [^{15}N]-labeled APC2 WHB alone (100 μM, red) or with UbV^{W_dim} (1:2, gold) with corresponding CSP analysis shown below (gold). (*A*, *Bottom*) Plots of CSPs (bar plots) for UbV^{W} and UbV^{W_dim} versus residue number. These results suggest similar interactions between APC2 WHB and the 2 UbVs. Proline residues are indicated with asterisks. (*B*) Overlaid 2-dimensional [^{15}N-^{1}H] HSQC spectra of UbV^{W} (black) and UbV^{W_dim} (red) at 308K. UbV^{W_dim} has more resonances resolvable than UbV^{W}, illustrating that this sample is more amenable to study by NMR. (*C*) Solution structures of UbV^{W_dim} bound to APC2 WHB confirm a domain-swapped dimer in solution, composed of ~67% of models that satisfy experimentally determined NOE constraints. All observed conformations of UbV^{W_dim} in the complex differ from all 3 previously observed crystal structures of domain-swapped dimer UbVs (UbV^{W}, UbV.XR, and UbV.15.D), confirming that hinge residues between protomer A (orange) and protomer B (blue) impart flexibility. However, all Ub-like fold "monomers" superimpose well with Ub (~1.3 Å root-mean-square deviation [RMSD] over Cα), and all populations show the same interaction between protomer A and the APC2 WHB domain. (*D*) Residues involved in the interaction between UbV^{W_dim} (orange and blue) and APC2 WHB (green) are illustrated as side chains originating from the ribbon structure. Arrows depict observed intermolecular NOEs in NMR experiments. (*E*) Model representation of the 3 observed interactions for APC2 WHB domain. (*E*) Representative structure of UbV^{W_dim} bound to APC2 WHB, compared with prior structures of UBE2C bound to APC2 WHB (Protein Data Bank [PDB] ID code 4YII [27]) (*Left*) and BUBR1 of the MCC bound to APC2 WHB from the MCC complex with APC/C^{CDC20} (PDB ID codes 5LCW [49] and 5KHU [48]) (*Right*). (*F*) Graphical illustration of the engineered UbV^{W_dim} "trap" designed to associate avidly with many components of APC/C. Coexpression of extended protomers of the UbV^{W_dim} enables multiple points of contact with APC/C. Protomer B of UbV^{W_dim} harbors an N-terminal D-box for recruitment to CDH1 and APC10, and a subsequent UbV^{R} moiety to bind APC11 RING domain. Protomer A of UbV^{W_dim} protomer has an N-terminal KEN-box to bind CDH1 and a C-terminal UBE2S-based extension for docking to APC/C platform subunits. (*G*, *Left*) An ~9-Å low-pass–filtered representation of a cryo-EM map of human APC/C^{CDH1} bound to the avid UbV^{W_dim} trap illustrates how UbV^{W_dim} associates with APC2 WHB. (*G*, *Top Right*) Cryo-EM map is overlaid with a prior map of APC/C^{CDH1}-Hsl1 D-box low-pass–filtered to a similar resolution (Electron Microscopy Data [EMD] accession code 2651 [25], green) reveals extra density. (*G*, *Bottom Right*) Docking of structures of UbV^{W} bound to APC2 WHB (orange and green, respectively) and UbV^{R} bound to APC11 RING (red and purple, respectively; PDB ID code 5JG6 [28]) shows how the additional EM density can be attributed to the avid UbV^{W_dim} trap.

(Fig. 4*D*). One end of the complex is secured by the UbV^{W} loop comprising Ala46 and Gly47 inserting in a hydrophobic groove between APC2 helices lined by Leu753, Tyr757, Phe780, Thr783, and Val803. The other edge is anchored by Leu73, Arg74, and Trp10 enwrapping the C terminus of the first APC2 WHB helix, through contacts with APC2's Gln759, Ala760, Met761, Thr763, and Asn764.

Many residues from the UbV^{W}-binding surface on APC2 were previously identified as contributing to the recruitment of UBE2C during substrate ubiquitylation, accounting for the inhibition of this reaction (Figs. 2*B* and 4*E*). Thus, the structure indicates that UbV^{W} inhibits substrate ubiquitylation by enveloping the surface of APC2 WHB responsible for recruiting UBE2C, competing with the binding of this E2 (27). Interestingly, 55% of APC2 residues contacted by the UbV^{W} also bind to the MCC in an APC/C^{CDC20}-MCC configuration that inhibits ubiquitylation during the spindle assembly checkpoint, before proper chromosome alignment on the mitotic spindle (48, 49) (Fig. 4 *D* and *E*).

We wished to confirm the UbV^{W_dim}-binding site within the full APC/C complex. However, previous studies showed that mobility of the APC2 WHB domain precludes its visualization in cryo-EM maps of APC/C, unless harnessed through multisite interactions (reviewed in ref. 51). For example, the APC2 WHB domain was best visualized in APC/C^{CDC20} bound to MCC, which naturally restricts flexibility through numerous interactions with multiple subunits in APC/C^{CDC20} (48, 49). It was also possible to visualize APC2's WHB domain in a structure representing substrate ubiquitylation, where an avid multisite binder mimicking the UBE2C-Ub substrate intermediate was generated by chemistry and protein engineering (27). On this basis, we engineered a complex in which UbV^{W_dim} was appended to additional sequences to avidly capture multiple mobile sites on APC/C^{CDH1} and visualize the interactions with APC2. Briefly, a KEN-box sequence from the substrate Hsl1 was encoded N-terminally to the original UbV sequence in UbV^{W_dim}, while a C-terminal UBE2S recruitment sequence would further anchor this protomer via interactions with the APC/C platform. The I44D mutant protomer B of UbV^{W_dim} was fused at the C terminus of a construct harboring the high-affinity D-box sequence from Hsl1, followed by the RING-binding UbV^{R} (Fig. 4*F*). This engineered UbV^{W_dim} complex, also containing multiple substrate and APC/C-binding elements, potently inhibits both UBE2C- and UBE2S-mediated APC/C reactions (*SI Appendix*, Fig. S2*D*), and by using it to purify recombinant APC/C^{CDH1}, we obtained a cryo-EM density map at an overall resolution of 6.6 Å. The overall map clearly resolves the majority of secondary structures, enabling fitting the corresponding regions of prior high-resolution structures of APC/C and CDH1. As expected, the APC2 WHB and APC11 RING domains were less well resolved. However, extra density corresponding to these domains and their associated UbVs is clearly observed upon downsampling the EM map to 9 Å and comparing it with the prior map of an APC/C^{CDH1} complex with the Hsl1 D-box peptide (25), in which the APC2 WHB and APC11 RING domains were not readily visible at this resolution (Fig. 4*G*). Although the resolution, together with similarity in the sizes of the 2 UbV complexes, precludes their definitive docking, it is possible to approximately place the structures of APC11 RING-UbV^{R} and APC2 WHB-UbV^{W} based on physical limitations imposed by their covalent linkage to other domains that are clearly resolved in the map. On this basis, the EM data show how the UbV^{W} can block UBE2C binding in the context of the fully assembled APC/C^{CDH1} complex (Fig. 4*G*). Notably, our engineered inhibitor acts much like the natural inhibitor MCC, by hijacking and reorienting APC2's mobile WHB domain.

APC2 WHB Is a Ub-Binding Domain. Because our prior studies of E3-targeting UbVs selected for tighter binders to known Ub-interacting sites on RING and HECT domains (21, 28, 42), we considered the converse possibility: Could UbV binding identify an unknown binding site on an E3? This question was addressed by NMR assays, whereby increasing concentrations of unlabeled Ub were titrated into a [^{15}N]-labeled version of the isolated APC2 WHB domain, and vice-versa. Indeed, [^{15}N-^{1}H] HSQC spectra showed that addition of high concentrations of Ub (500 μM titrant shown) caused chemical shift perturbations at the UbV-binding surface of APC2's WHB domain (Fig. 5*A*). Concordantly, the APC2 WHB domain elicited chemical shift perturbations of the hydrophobic surface on Ub (*SI Appendix*, Fig. S3 *A* and *B*). Thus, the APC2 WHB domain is a Ub-binding domain.

APC2 WHB Preferentially Binds K48-Linked Ub Chains. Does APC2's WHB domain preferentially bind a particular type of Ub chain? To address this question, we first purified linkage-specific di-Ub conjugates (*SI Appendix*, Fig. S3*C*) for 3 architectures: K11 and K48 chains, based on human APC/C producing these linkages, and K63 chains, which are not recognizable components of APC/C-dependent signaling but are highly abundant in cells. Chemical shift perturbations were monitored in [^{15}N-^{1}H] HSQC spectra of the [^{15}N]-labeled APC2 WHB domain upon titrating each of these chains (Fig. 5*B*), but only the conjugates harboring a K48 linkage elicited greater chemical shift perturbations relative to the effects of Ub alone (Fig. 5 *C*–*E* and *SI Appendix*, Fig. S3*D*). Notably, the isolated RING domain exhibited no preference for any chain linkage type under identical experimental conditions (*SI Appendix*, Fig. S3 *E*–*G*), highlighting the specificity of K48 di-Ub's association with the APC2 WHB domain.

We wished to obtain insights into how K48-linked di-Ub might preferentially bind the APC2 WHB domain, although we were unable to obtain a structure of a complex with a Ub chain, possibly due to intramolecular competition for WHB binding or a slight collateral restructuring of Ub-binding sites evidenced in Cα deviations for this region upon UbV^{W} titration (*SI Appendix*, Fig. S4*A*). It seems likely that one Ub binds in a manner similar to the UbV^{W_dim}, because the few resonances that shift upon binding the K48-linked di-Ub all correspond to residues at the interface in the APC2/UbV^{W_dim} complex. Thus, a potential placement for one Ub can be modeled by grafting Ub in place of the main Ub fold from UbV^{W_dim}. A possible model for the second Ub was provided by a fortuitous 2.2-Å resolution crystal structure of a single Ub bound to APC2's WHB domain (Fig. 5*F* and *SI Appendix*, Table S1). In the crystal, Ub's C terminus points toward the UbV/E2-binding surface and its hydrophobic patch mediates interactions via an APC2 surface involving Arg778, Val782, Pro785, Ala786, Ala788, and Glu789. This interaction differs from the main contacts revealed by NMR and is presumably stabilized by crystal contacts supported by the high protein concentrations that occur during crystallization. Notably, the primary Ub-binding site observed by NMR is shielded by crystal contacts. Nonetheless, the distances measured between the C-terminal residue visible in the crystal (Leu73) and each lysine in the modeled primary-binding Ub provide a potential rationale for the linkage preference for conjugate binding: Only a K48-linked Ub chain would be compatible with this di-Ub arrangement (Fig. 5*G*). Consistent with our hypothesis, ubiquitylation of substrate (*SI Appendix*, Fig. S4*B*) leads to a less productive E2 encounter monitored by the rate of discharge of Ub from the catalytic cysteine of UBE2C in the presence of APC/C^{CDH1} (*SI Appendix*, Fig. S4*C*), although future studies will be required to definitively determine the basis for this reduced activity, the structural details for K48-linked Ub chain binding to APC2, and the functions of these interactions.

Discussion

UbVs are emerging as powerful tools for probing functions of the Ub system. To date, we and others have selected for UbVs

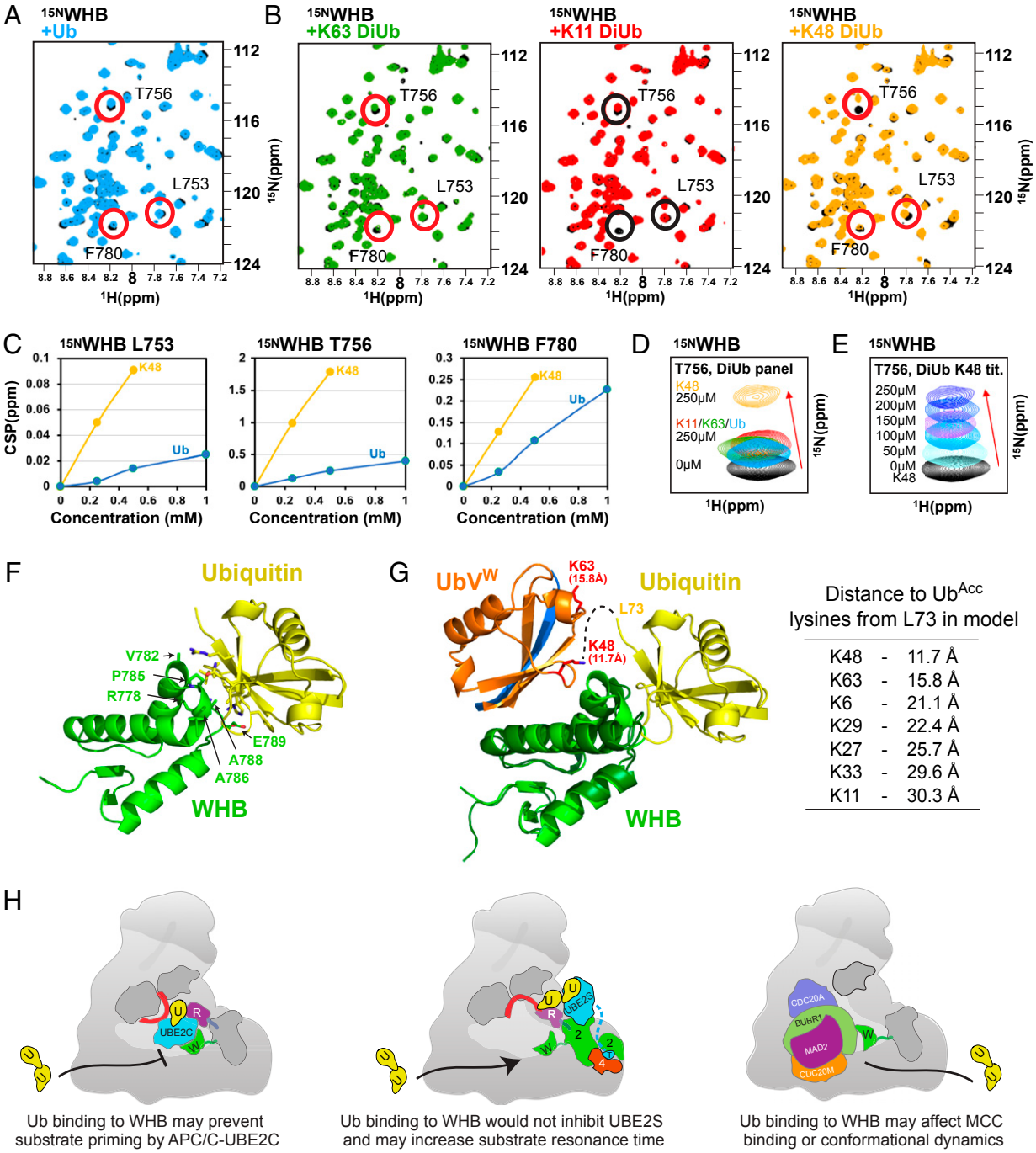

Fig. 5. APC2 WHB domain binds Ub conjugates linked by K48. (*A*) Overlaid [^{15}N-^{1}H] HSQC spectra of [^{15}N]-labeled APC2 WHB alone (200 μM, black) or with Ub (1:2.5, light blue). Ub itself causes minor chemical shifts of the APC2 WHB spectra, including for residues L753, T756, and F780, which associate with UbV^{W} in Fig. 4. (*B*) Overlaid [^{15}N-^{1}H] HSQC spectra of [^{15}N]-labeled APC2 WHB alone (200 μM, black) or with purified, enzymatically assembled di-Ubs of distinct linkages. (*B*, *Left*) K63 di-Ub (250 μM, green). (*B*, *Middle*) K11 di-Ub (250 μM, red). (*B*, *Right*) K48 di-Ub (250 μM, gold). (*C*) CSP values at the indicated residues are plotted for titrations of K48-linked di-Ub and purified Ub. Titration of K48 di-Ub causes a greater chemical shift than Ub alone. (*D*) Chemical shift perturbations observed for residue T756 at the Ub-APC/C interface for different forms of Ub. The titrants and concentrations are marked. (*E*) Chemical shift perturbations observed for residue T756 at the Ub-APC/C interface for titrations of K48-linked di-Ub. The titrant concentrations are marked. (*F*) A 2.2-Å crystal structure of Ub bound to isolated APC2 WHB domain. Distinct residues of APC2 are observed associating with Ub, including V782, P785, R778, E789, A788, and A786. (*G*, *Left*) Superimposition over the APC2 WHB domain of the crystal structure and solution structures reveals 2 distinct locations for Ub-like molecules to associate with APC. Dashed lines indicate a possible trajectory for 3 remaining C-terminal residues of Ub to form a K48-linked chain. (*G*, *Right*) Distances to each side-chain lysine of Ub are measured from Leu73 of the donor Ub in the shown model and listed ascendingly. (*H*) Cartoon model demonstrating potential functional consequences of Ub~WHB interaction. (*H*, *Left*) Ub chain association with WHB could compete for UBE2C recruitment to APC/C, inhibiting ubiquitylation of substrate lysines. (*H*, *Middle*) Ub recruitment to APC2 WHB could enhance UBE2S activities in multiple ways: Here, substrates are retained longer on APC/C, while UBE2S would also have unhindered access to APC/C with the UBE2C-binding site blocked. (*H*, *Right*) Ub association with WHB could have multiple potential effects on MCC association with APC/C. The Ub chain may compete with BUBR1 for contacting WHB. Disrupting the MCC–WHB interaction could lead to an alternate conformation or aid in MCC dissociation from APC/C. Alternatively, harboring Ub that is conjugated directly to MCC could further affect the conformational landscape and limit dissociation of the inhibitor itself.

that bind catalytic domains from enzymes (DUBs, E3 ligases, and E2-conjugating enzymes), interchangeable cullin-binding subcomplexes (Skp1–F-box proteins), and Ub-binding domains (21, 28, 38–44). These selections have yielded hundreds of tools targeting the known domains by modulating catalytic activity and assembly of E3 ligases and inhibiting Ub binding by well-recognized interacting domains. Here, we identified a UbV-modulating activity of the massive, multifunctional RING E3 ligase, APC/C, through an entirely different route: scanning through a panel of purified UbVs for effects on in vitro ubiquitylation (Fig. 1*B*). Remarkably, even a relatively small collection of UbVs contained a UbV (UbV^W) with a distinct mode of action, selectively inhibiting ubiquitylation by only a single E2 of the 2 E2s associated with APC/C. Importantly, UbV^W also inhibits APC/C-dependent substrate turnover in the ex vivo setting of mitotic extracts from *Xenopus* eggs (Fig. 1*F*). Mechanistic and structural studies revealed that unlike other characterized UbV inhibitors of ubiquitylation, UbV^W does not bind a hallmark E3 ligase catalytic domain. Rather, UbV^W blocks an auxiliary site, the WHB domain from APC/C's APC2 subunit, from selecting and positioning UBE2C for substrate priming (Figs. 2 and 4). E2 specificity was achieved because this APC2 domain is dispensible for APC/C's other partner E2, UBE2S, provided that substrates are premarked with a Ub for chain elongation. Interestingly, an emerging theme in E2/E3 interactions is the importance of secondary interactions beyond hallmark RING domains in establishing specificity. Thus, our results raise the possibility that UbVs may generally be useful tools for targeting such auxiliary interactions to selectively modulate only subsets of E3 activities. In terms of UbV^W, we envision that more directed studies in the future could be used to select for tighter binding UbVs that target APC's WHB domain, which could serve as affinity probes for cell-based studies aimed at understanding biological roles of UBE2C.

UbV^W also guided our unanticipated identification of APC2's WHB domain as a Ub-binding domain in APC/C (Fig. 5). Reasoning that UbVs preserve many key features of the Ub fold, and that the majority of UbVs studied to date interact with known Ub-binding sites, we tested for Ub binding by NMR. The limited chemical shift changes at high protein concentrations likely reflect extremely weak interactions. Such weak binding is on the same scale as Ub interactions with other well-characterized, validated partners. This includes APC11's RING domain, which recruits a free Ub with a K_m in the millimolar range for UBE2S-dependent K11-linked chain formation (22). It is thought that weak Ub interactions are important for contributing, as one of several elements, to multisite interactions (36, 37). Several protein–protein interactions that are weak on their own can synergize to produce high local concentrations sufficient for binding with high specificity. Such interactions are also dynamic, because binding is achieved through avidity of many simultaneous interactions, while disruption of any individual interaction could be sufficient to dismantle an assembly. Another explanation for low affinity is to prevent errantly blocking an individual Ub-binding site by the massive amount of Ub present in noncognate contexts.

In terms of Ub binding to APC2's WHB domain, several scenarios could establish avidity. In addition to K48-linked chains that could bind to APC2, ubiquitylated APC/C substrates harbor 1 or more distinct degrons interacting with a coactivator (reviewed in ref. 52). Ubiquitylation could also modulate binding of APC/C regulators, such as the MCC. Another source of avidity may arise from multiple Ubs linked to each other and/or to different sites on substrates. Indeed, a K48-linked conjugate (i.e., harboring 2 Ubs) shows increased interaction with APC2's WHB domain (Fig. 5 *C* and *D*), while additional substrate-linked Ubs could potentially capture the Ub-binding exosite on APC11's RING domain (22, 28). Notably, our cryo-EM map enabling the visualization of APC/C interactions with UbV^{W_dim} relied on conceptually related multisite interactions also involving 2 substrate degrons and 2 APC/C-binding elements (Fig. 4*G*).

As with many functionally important Ub-binding exosites upon their initial discovery (53–55), the roles of Ub binding to APC2's WHB domain remain unknown. Although the requirement for this same surface for substrate ubiquitylation imposes technical challenges for studying function, it also implies potential roles, either antagonizing UBE2C or participating in UBE2C-independent activities. One such activity is polyubiquitylation by UBE2S after UBE2C-dependent priming. In principle, APC2's WHB domain could capture emerging K48-linked chains on substrates, increasing a substrate's lifetime on APC/C and thereby the potential for UBE2S-dependent modification with K11-linked chains. This could also contribute to switching between the two E2 activities, or modulating binding of the MCC (Fig. 5*H*). Although it is presently unknown whether UBE2C and UBE2S can function simultaneously or not on a single APC/C complex, if ubiquitylation by the 2 E2s is mutually exclusive, then Ub binding to APC2's WHB domain would block UBE2C and thereby enable K11-linked chain formation by UBE2S. APC2's WHB domain could also contribute to localizing APC/C to particular subcellular localizations harboring K48-linked chains or chain-forming activity. It is compelling that these mechanisms could all contribute to marking of substrates with both K48 and K11 linkages, a feature of APC/C substrates recently shown to direct their 26S proteasomal degradation (33, 56).

Finally, our study demonstrates that UbV technology can identify Ub-binding sites within massive multiprotein complexes. As UbVs are traditionally selected in binding assays, much like the generation of other affinity reagents through phage or other display technologies, it seems likely that use of entire assemblies even in the megadalton range could be used to discover UbVs. However, UbV^W was instead identified through an enzymatic assay (Fig. 1*B*). Thus, extending the modalities by which UbVs could be expressed and selected, for example, through expression in pools, could be useful for identifying UbVs that mimic myriad functions of Ub binding. We envision numerous ways one could affect in vitro ubiquitylation depending on the order of addition of reaction components, including through modulating multiprotein complex E3 assembly, substrate binding, E2 binding, Ub ligation, ubiquitylated substrate binding, and linkage specificity of polyubiquitylation. Such approaches may be particularly useful for identifying cryptic Ub-binding sites regulating dynamic multifunctional E3s like APC/C. Although we have now identified several exosites, on the APC11 RING domain and on the APC2 WHB domain, these do not completely eliminate processivity of multiubiquitylation and polyubiquitylation by UBE2C, indicating that additional Ub-binding sites on APC/C remain to be discovered (22, 28, 34, 35). It seems like other massive molecular machines in the Ub system, including the 26S proteasome, many E3s and their associated E2s, will emerge to be highly regulated through numerous Ub-binding sites acting in concert and yet dynamically to modulate function (5, 7, 37). We thus anticipate massive capabilities for UbVs to both unearth and target these sites to transform our understanding of roles of Ub in regulation.

Materials and Methods

Recombinant APC/C, CDH1, and UBA1 were expressed in High Five insect cells and all other proteins in *Escherichia coli* as described previously (22, 28). The complex "trap" for visualizing UbV^W binding to APC2 WHB in the context of the full APC/C^{CDH1} complex was the product of coexpression of 2 gene products encoding several APC/C^{CDH1}-binding moieties; more details are available in *SI Appendix*. Ubiquitylation reactions, NMR, and substrate degradation assays in *Xenopus laevis* egg extracts were largely performed as described previously (22, 28). Crystallographic data were collected at Advanced Photon Source Northeastern Collaborative Access Team ID-24-C and Southeast Regional Collaborative Access Team ID-22 beamlines. Further details can be found in *SI Appendix*.

ACKNOWLEDGMENTS. We thank Dr. J. Kellermann, Dr. S. Uebel, Dr. K.-P. Wu, M. Zobawa, and M. Brunner for their scientific and technical advice. We are grateful to Dr. M. Strauss for training and assistance with the cryo-EM experiments. We thank Dr. V. Chau and Dr. C. Coleman for the GP78-UBC7 plasmid used for the generation of K48-linked di-Ub. This study received funding from the CRS Scholarship for the Next Generation of Scientists (to W.Z.); Deutsche Forschungsgemeinschaft Sonderforschungsbereich 860 (to H.S.); Boehringer Ingelheim; Austrian Research Promotion Agency (Forschungsförderungsgesellschaft Laura Bassi Centre for Optimized Structural Studies); European Union (Seventh Framework Programme Grant 227764 MitoSys); Austrian Science Fund (Grant SFB-F34 and Wittgenstein award to J.-M.P.); NIH Grant R35GM128855 and University Cancer Research Fund (to N.G.B.); Genome Canada Disruptive Innovation in Genomics Grant OGI-119 (to S.S.S.); and American Lebanese Syrian Associated Charities, Howard Hughes Medical Institute, NIH Grants R37GM065930 and P30CA021765 (to B.A.S.).

1. L. Buetow, D. T. Huang, Structural insights into the catalysis and regulation of E3 ubiquitin ligases. *Nat. Rev. Mol. Cell Biol.* **17**, 626–642 (2016).
2. F. Mattiroli, T. K. Sixma, Lysine-targeting specificity in ubiquitin and ubiquitin-like modification pathways. *Nat. Struct. Mol. Biol.* **21**, 308–316 (2014).
3. N. Zheng, N. Shabek, Ubiquitin ligases: Structure, function, and regulation. *Annu. Rev. Biochem.* **86**, 129–157 (2017).
4. L. Randles, K. J. Walters, Ubiquitin and its binding domains. *Front. Biosci.* **17**, 2140–2157 (2012).
5. I. Dikic, S. Wakatsuki, K. J. Walters, Ubiquitin-binding domains - from structures to functions. *Nat. Rev. Mol. Cell Biol.* **10**, 659–671 (2009).
6. K. Husnjak, I. Dikic, Ubiquitin-binding proteins: Decoders of ubiquitin-mediated cellular functions. *Annu. Rev. Biochem.* **81**, 291–322 (2012).
7. D. Komander, M. Rape, The ubiquitin code. *Annu. Rev. Biochem.* **81**, 203–229 (2012).
8. E. Oh, D. Akopian, M. Rape, Principles of ubiquitin-dependent signaling. *Annu. Rev. Cell Dev. Biol.* **34**, 137–162 (2018).
9. K. K. Dove, R. E. Klevit, RING-Between-RING E3 ligases: Emerging themes amid the variations. *J. Mol. Biol.* **429**, 3363–3375 (2017).
10. H. Walden, K. Rittinger, RBR ligase-mediated ubiquitin transfer: A tale with many twists and turns. *Nat. Struct. Mol. Biol.* **25**, 440–445 (2018).
11. V. Fajner, E. Maspero, S. Polo, Targeting HECT-type E3 ligases–Insights from catalysis, regulation and inhibitors. *FEBS Lett.* **591**, 2636–2647 (2017).
12. S. Lorenz, Structural mechanisms of HECT-type ubiquitin ligases. *Biol. Chem.* **399**, 127–145 (2018).
13. F. C. Streich, Jr, C. D. Lima, Structural and functional insights to ubiquitin-like protein conjugation. *Annu. Rev. Biophys.* **43**, 357–379 (2014).
14. M. B. Metzger, J. N. Pruneda, R. E. Klevit, A. M. Weissman, RING-type E3 ligases: Master manipulators of E2 ubiquitin-conjugating enzymes and ubiquitination. *Biochim. Biophys. Acta* **1843**, 47–60 (2014).
15. D. C. Scott *et al*., Two distinct types of E3 ligases work in unison to regulate substrate ubiquitylation. *Cell* **166**, 1198–1214.e24 (2016).
16. M. C. Rodrigo-Brenni, S. A. Foster, D. O. Morgan, Catalysis of lysine 48-specific ubiquitin chain assembly by residues in E2 and ubiquitin. *Mol. Cell* **39**, 548–559 (2010).
17. K. Wu, J. Kovacev, Z. Q. Pan, Priming and extending: A UbcH5/Cdc34 E2 handoff mechanism for polyubiquitination on a SCF substrate. *Mol. Cell* **37**, 784–796 (2010).
18. J. D. Wright, P. D. Mace, C. L. Day, Noncovalent ubiquitin interactions regulate the catalytic activity of ubiquitin writers. *Trends Biochem. Sci.* **41**, 924–937 (2016).
19. A. Patel, G. J. Sibbet, D. T. Huang, Structural insights into non-covalent ubiquitin activation of the cIAP1-UbcH5B~ubiquitin complex. *J. Biol. Chem.* **294**, 1240–1249 (2019).
20. L. Buetow *et al*., Activation of a primed RING E3-E2-ubiquitin complex by non-covalent ubiquitin. *Mol. Cell* **58**, 297–310 (2015).
21. W. Zhang *et al*., System-wide modulation of HECT E3 ligases with selective ubiquitin variant probes. *Mol. Cell* **62**, 121–136 (2016).
22. N. G. Brown *et al*., Mechanism of polyubiquitination by human anaphase-promoting complex: RING repurposing for ubiquitin chain assembly. *Mol. Cell* **56**, 246–260 (2014).
23. I. Primorac, A. Musacchio, Panta rhei: The APC/C at steady state. *J. Cell Biol.* **201**, 177–189 (2013).
24. S. Sivakumar, G. J. Gorbsky, Spatiotemporal regulation of the anaphase-promoting complex in mitosis. *Nat. Rev. Mol. Cell Biol.* **16**, 82–94 (2015).
25. L. F. Chang, Z. Zhang, J. Yang, S. H. McLaughlin, D. Barford, Molecular architecture and mechanism of the anaphase-promoting complex. *Nature* **513**, 388–393 (2014).
26. L. Chang, Z. Zhang, J. Yang, S. H. McLaughlin, D. Barford, Atomic structure of the APC/C and its mechanism of protein ubiquitination. *Nature* **522**, 450–454 (2015).
27. N. G. Brown *et al*., RING E3 mechanism for ubiquitin ligation to a disordered substrate visualized for human anaphase-promoting complex. *Proc. Natl. Acad. Sci. U.S.A.* **112**, 5272–5279 (2015).
28. N. G. Brown *et al*., Dual RING E3 architectures regulate multiubiquitination and ubiquitin chain elongation by APC/C. *Cell* **165**, 1440–1453 (2016).
29. H. Yu, R. W. King, J. M. Peters, M. W. Kirschner, Identification of a novel ubiquitin-conjugating enzyme involved in mitotic cyclin degradation. *Curr. Biol.* **6**, 455–466 (1996).
30. M. J. Garnett *et al*., UBE2S elongates ubiquitin chains on APC/C substrates to promote mitotic exit. *Nat. Cell Biol.* **11**, 1363–1369 (2009).
31. A. Williamson *et al*., Identification of a physiological E2 module for the human anaphase-promoting complex. *Proc. Natl. Acad. Sci. U.S.A.* **106**, 18213–18218 (2009).
32. T. Wu *et al*., UBE2S drives elongation of K11-linked ubiquitin chains by the anaphase-promoting complex. *Proc. Natl. Acad. Sci. U.S.A.* **107**, 1355–1360 (2010).
33. H. J. Meyer, M. Rape, Enhanced protein degradation by branched ubiquitin chains. *Cell* **157**, 910–921 (2014).
34. Y. Lu, W. Wang, M. W. Kirschner, Specificity of the anaphase-promoting complex: A single-molecule study. *Science* **348**, 1248737 (2015).
35. A. Kelly, K. E. Wickliffe, L. Song, I. Fedrigo, M. Rape, Ubiquitin chain elongation requires E3-dependent tracking of the emerging conjugate. *Mol. Cell* **56**, 232–245 (2014).
36. L. Hicke, H. L. Schubert, C. P. Hill, Ubiquitin-binding domains. *Nat. Rev. Mol. Cell Biol.* **6**, 610–621 (2005).
37. F. Liu, K. J. Walters, Multitasking with ubiquitin through multivalent interactions. *Trends Biochem. Sci.* **35**, 352–360 (2010).
38. W. Zhang *et al*., Generation and validation of intracellular ubiquitin variant inhibitors for USP7 and USP10. *J. Mol. Biol.* **429**, 3546–3560 (2017).
39. N. Manczyk *et al*., Structural and functional characterization of a ubiquitin variant engineered for tight and specific binding to an alpha-helical ubiquitin interacting motif. *Protein Sci.* **26**, 1060–1069 (2017).
40. H. Huang *et al*., E2 enzyme inhibition by stabilization of a low-affinity interface with ubiquitin. *Nat. Chem. Biol.* **10**, 156–163 (2014).
41. M. Gorelik *et al*., A structure-based strategy for engineering selective ubiquitin variant inhibitors of Skp1-Cul1-F-box ubiquitin ligases. *Structure* **26**, 1226–1236.e3 (2018).
42. M. Gabrielsen *et al*., A general strategy for discovery of inhibitors and activators of RING and U-box E3 ligases with ubiquitin variants. *Mol. Cell.* **68**, 456–470.e10 (2017).
43. A. Ernst *et al*., A strategy for modulation of enzymes in the ubiquitin system. *Science* **339**, 590–595 (2013).
44. Y. Zhang *et al*., Conformational stabilization of ubiquitin yields potent and selective inhibitors of USP7. *Nat. Chem. Biol.* **9**, 51–58 (2013).
45. S. Vijay-Kumar, C. E. Bugg, W. J. Cook, Structure of ubiquitin refined at 1.8 Å resolution. *J. Mol. Biol.* **194**, 531–544 (1987).
46. R. W. King *et al*., A 20S complex containing CDC27 and CDC16 catalyzes the mitosis-specific conjugation of ubiquitin to cyclin B. *Cell* **81**, 279–288 (1995).
47. H. Yamano, J. Gannon, H. Mahbubani, T. Hunt, Cell cycle-regulated recognition of the destruction box of cyclin B by the APC/C in Xenopus egg extracts. *Mol. Cell* **13**, 137–147 (2004).
48. M. Yamaguchi *et al*., Cryo-EM of mitotic checkpoint complex-bound APC/C reveals reciprocal and conformational regulation of ubiquitin ligation. *Mol. Cell* **63**, 593–607 (2016).
49. C. Alfieri *et al*., Molecular basis of APC/C regulation by the spindle assembly checkpoint. *Nature* **536**, 431–436 (2016).
50. J. Teyra *et al*., Structural and functional characterization of ubiquitin variant inhibitors of USP15. *Structure* **27**, 590–605.e5 (2019).
51. E. R. Watson, N. G. Brown, J. M. Peters, H. Stark, B. A. Schulman, Posing the APC/C E3 ubiquitin ligase to orchestrate cell division. *Trends Cell Biol.* **29**, 117–134 (2019).
52. N. E. Davey, D. O. Morgan, Building a regulatory network with short linear sequence motifs: Lessons from the degrons of the anaphase-promoting complex. *Mol. Cell* **64**, 12–23 (2016).
53. P. S. Brzovic, A. Lissounov, D. E. Christensen, D. W. Hoyt, R. E. Klevit, A UbcH5/ubiquitin noncovalent complex is required for processive BRCA1-directed ubiquitination. *Mol. Cell* **21**, 873–880 (2006).
54. H. C. Kim, A. M. Steffen, M. L. Oldham, J. Chen, J. M. Huibregtse, Structure and function of a HECT domain ubiquitin-binding site. *EMBO Rep.* **12**, 334–341 (2011).
55. E. Maspero *et al*., Structure of the HECT:ubiquitin complex and its role in ubiquitin chain elongation. *EMBO Rep.* **12**, 342–349 (2011).
56. R. G. Yau *et al*., Assembly and function of heterotypic ubiquitin chains in cell-cycle and protein quality control. *Cell* **171**, 918–933.e20 (2017).